Curvature Based Analysis of Handwritten Symbols

Kim Man Lui†, Anton D. Brink‡ and Michael Sears‡

†Department of Computer Science, University of the Witwatersrand, Johannesburg, South Africa

‡Department of Computational and Applied Mathematics, University of the Witwatersrand Johannesburg, South Africa

Pattern recognition is an important branch of computer vision and intelligent robotics. This paper explores local curve theory for different pattern recognition applications: recognition of good handwritten symbols (Fig 1), analysis of the hierarchical structure of 2-D patterns and simple 3-D object recognition. In the case of 2-D patterns, our technique is compared with a recent related method based on generalized Hough transforms and it is found that it is more robust with respect to complex image outlines.

1. Introduction

An understanding of the properties of curves and surfaces based on differential geometry can be used as an aid to visualization and recognition of simple image patterns. In the past, geometry has been applied to different aspects of computer graphics and image processing. However, the simplest application of differential geometry is the study of curves and surfaces in both local and global views. 2D–patterns and 3D–objects are always discerned by the human observer in terms of their geometric characteristics. For example, a triangle is perceived as the end points of three lines linked with each other. This implies that it must have three angles. Therefore if a pattern has three vertices, one may claim that it is a triangle (Fig 1).

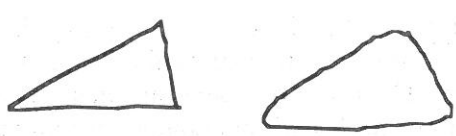

Fig. 1. We claim that these two handwritten triangles are well defined, because their differential structures have a weak likeness.

A closed regular curve defines the shape of an image, resembling a silhouette (Fig 2). Thus a simple pattern can be determined by means of its silhouette. The problem then reverts to silhouette recognition by the description of its outline.

Fig. 2. Image of A Silhouette of A

Before the theoretical discussion, it is of some interest to note a related phenomenon that occurs in daily life. When a vehicle travels along a closed path with constant speed, the driver can determine the shape of the path. For example, he would feel a constant centripetal force if it is a circle, or he could determine that it is an S shape if he arrives back at the starting point after experiencing a centripetal force changing direction four times (Fig 3), from side to side. In the case of a 3-D spatial orbit, this concept can clearly be extended to 3-D object recognition.

The paper proceeds as follows: In the next section, we introduce the mathematical underpinnings of 2-D recognition. This formalism is also used for 3-D recognition. Section 3 illus-

Fig. 3. $*$ marks the points at which centripetal force changes direction.

trates how the method recognizes handwritten symbols with results of implementation. In section 4, we discuss the generalized Hough Transforms and related difficulties in distinguishing very complex image outlines. Section 5 extends the formalism to 3-D object recognition. 3-D object recognition is generally more complex than 2-D methods. The proposed method attempts to link common characteristics of the 2D and 3D recognition problems. However, the paper focuses mainly on 2D methods. The final section presents our conclusions.

2. A Geometric Property of the Image Set

2.1 Image Outline

The boundary of an image pattern is a simple closed curve $\mathbf{f}(t) = (x(t), y(t))$, called the *image outline*. Thus, $\mathbf{f}$ is a closed curve of period q with $\mathbf{f}(p_1) = \mathbf{f}(p_2)$ if and only if $p_1 - p_2 = nq$ for all integers n and q is the smallest positive number with this property. The function $\mathbf{f} : [p_1, p_1 + q) \to \mathbf{R}^2$ is an embedding. In fact, the curve is an immersion; that is, it satisfies $\mathbf{f}'(t) = d\mathbf{f}/dt \neq 0, \forall t \in [p_1, p_1 + q]$.

To tackle the problem of different image sizes and scales a reparameterization of a curve is necessary. For an image outline α, the arc–length function $s : [p_1, p_1 + q] \to \mathbf{R}$,

$$s(t) = \int_{p_1}^{p_1+t} |\alpha'(u)| du, \quad \text{for } 0 \leq t \leq q$$

is a diffeomorphism $s : [p_1, p_1 + q] \to [0, S]$, where S is the length of α. (A differentiable map $\Psi : M \to N$ is a diffeomorphism if there is a differentiable map $\Phi : N \to M$ such that $\Phi \circ \Psi = I$ and $\Psi \circ \Phi = I$, where I is an identity).

Thus the image outline $\mathbf{f} = \alpha^{-1}$ is parameterized by arc length of α, so $s = \int_0^s \left|\frac{d\mathbf{f}}{d\omega}\right| d\omega$ for $s \in [0, S]$. By the fundamental theorem of calculus, we have

$$1 = \frac{d}{ds}\int_0^s \left|\frac{d\mathbf{f}}{d\omega}\right| d\omega = \left|\frac{d\mathbf{f}}{d\omega}\right| \text{ at } \omega = s,$$

that is,

$$1 = \left|\frac{d\mathbf{f}}{ds}\right|$$

Thus the velocity vector field $d\mathbf{f}/ds$ is a unit vector field along the outline, as it $\mathbf{T}$, where $\mathbf{T}$ is the unit vector in the direction of the velocity vector.

A curve $\mathbf{f} : (a, b) \to \mathbf{R}^2$ is unit speed if $|d\mathbf{f}/dt| = 1$. For a unit speed curve $\mathbf{f} = \mathbf{f}(t)$, the arc length is $t - t_0$. Above t_0 was chosen to be 0 (so that $s = t$) and we can write $\mathbf{f}$ as a function of s. Any regular curve can be reparameterized and this does not change the geometric property of a curve since each image outline can be expressed in terms of a unit speed curve. Its tangent vector field is a geometric property.

Theorem. *Let* $\mathbf{f} : (a, b) \to \mathbf{R}^2$ *be regular curve and let* $g : (c, d) \to (a, b)$ *be a reparameterization. Define* $\mathbf{h} = \mathbf{f} \circ g$. *If* $t_0 = g(r_0)$, *the tangent vector field* $\mathbf{T}$ *of* $\mathbf{f}$ *at* t_0 *and the tangent vector field* $\mathbf{S}$ *of* $\mathbf{h}$ *at* r_0 *satisfy* $\mathbf{S} = \pm\mathbf{T}$.

Proof.

$$\begin{aligned}\mathbf{S} &= (d\mathbf{h}/dr)/(|d\mathbf{h}/dr|) \\ &= (d\mathbf{f}/dt)(dg/dr)/(|d\mathbf{f}/dt||dg/dr|) \\ &= \mathbf{T} \cdot (\pm 1) = \pm\mathbf{T}.\end{aligned}$$

If $dg/dr > 0$, it means that particles are moving along the image curve in the same direction; if $dg/dr < 0$, they move in opposite directions.

2.2 Interpretation of the Image Set

Curvature defined as $\kappa(s) = |\mathbf{T}'(s)|$ in a unit speed curve $\mathbf{f}(s)$ measures the amount of curvature. Thus if two image outlines are similar, their rates of directional change of tangent field must be similar as well. This can be determined from the principal normal vector field. (Note: Stein and Medioni (1992) reported their method of structural indexing. This is similar to our

method, besed on the utilization of geometric features of the image outline. The basic difference is that structural indexing looks for the change of angle between neighboring segments, not a complete image outline).

Definition. The principal normal vector field to a unit speed curve $\mathbf{f}(s)$ is the unit vector field $\mathbf{N}(s) = \mathbf{T}'(s)/\kappa(s)$. The binormal vector field to $\mathbf{f}(s)$ is $\mathbf{B}(s) = \mathbf{T}(s) \times \mathbf{N}(s)$. The torsion of $\mathbf{f}$ is the real–valued function $\tau(s) = -\mathbf{B}'(s) \cdot \mathbf{N}(s)$.

Since the image outline is immersed in a plane, $\tau(s) = 0$. Suppose there are two outlines $\mathbf{f}_1$ and $\mathbf{f}_2$. Note that the outlines may be different sizes, but they must be reparameterized. Let $\varepsilon(s)$ be a real–valued function describing a threshold for a group of similar images; in some cases $\varepsilon(s)$ could be a constant function. Thus the images belong to the same group if $|\mathbf{N}_1(s) - \mathbf{N}_2(s)| < \varepsilon(s)$. However, the formula only considers a point, not the neighborhood of a point on the outline. So let δ be a real constant. Two images are similar to each other if, for each s_1, there exists s_2 such that $|\mathbf{N}_1(s_1) - \mathbf{N}_2(s_2)| < \varepsilon(s)$ and $|s_1 - s_2| < \delta$ where s_1, s_2 belong to the domains of two outlines $\mathbf{f}_1$ and $\mathbf{f}_2$, respectively.

In Fig 4, suppose $\varepsilon(s)$ is a constant. Clearly, this is incorrect if $|\mathbf{N}_1(s) - \mathbf{N}_2(s)| < \varepsilon(s)$ at point $s = p$ and $s = q$. Therefore $\varepsilon(s)$ should be defined as:

$$\varepsilon(s) = \begin{cases} \varepsilon_1, & \text{if } s \in (p-\delta, p+\delta), \\ \varepsilon_2, & \text{if } s \in (q-\delta, q+\delta), \\ \varepsilon_3, & \text{otherwise,} \end{cases}$$

where $\delta, \varepsilon_1, \varepsilon_2$ and ε_3 are real constants.

These values form a set of thresholds for taking a decision about whether an image outline matches the symbol "$\vee$".

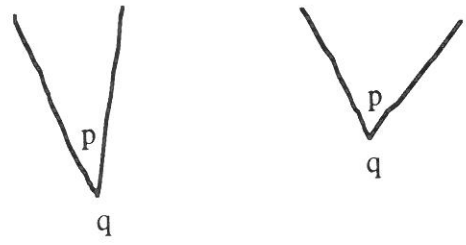

Fig. 4. It is obvious that $|\mathbf{N}_1(s) - \mathbf{N}_2(s)| <$ constant, except in the neighborhoods of points p and q.

Alternatively, analysis of the local minima and maxima on $x(s)$ and $y(s)$, $\mathbf{f} = (x(s), y(s))$, yields the number of convex segments (Fig 5). This can be done using $\mathbf{f}'(s)$ and $\mathbf{f}''(s)$. A convex segment is a finite curve such that it lies on one side of each tangent line. Convex segments provide no information about directional change along a curve, and thus it is necessary to note the position of each convex segment on $\mathbf{f}(s)$. This follows a similar principle to the above and simplifies implementation.

Apart from the rate of change of the tangent vector, a global property of curves that also involves local curves is related to the derivative of curvature. A vertex of a curve is a point such that $\kappa'(s) = 0$. Clearly a circle has no vertices. However, a non–circular ellipse has exactly four vertices, these being the points where κ has a local maximum or minimum (Spivak 1979).

Recognition of a simple handwritten "A" is considered in Fig 6. An *image outline vertex* is defined as a point s such that $\kappa(s) > \phi$ and $\kappa'(s) < \phi$, where $\kappa(s)$ is the curvature of the outline (the definition differs from Spivak 1979) and ϕ is a threshold value for the determination of a vertex. Clearly, an "A" has 5 outline vertices. Each segment curve of the "A" between

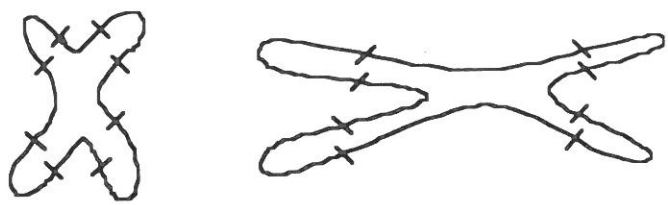

Fig. 5. Convex segments provide partial information about the image outline.

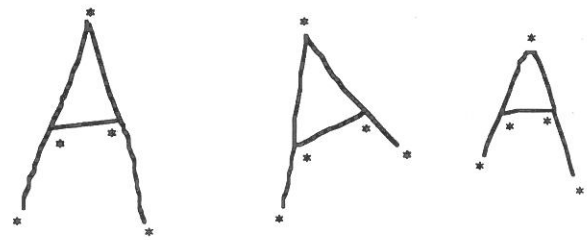

Fig. 6. Samples of a handwritten "A". Symbol * indicates the outline vertices.

two vertices has to be reparameterized by s such that the length is 1 unit. The aim is to standardize all segments of the image outline of "A" so that corresponding segments can be compared. Note that the unit lengths of segments within a single shape cannot be compared. Our main concern is with differential structure. Afterwards, the whole image outline is reparameterized again by the total unit length, and the problem reverts to the one in Fig 4, i. e. to find the threshold function $\varepsilon(s)$ for a group of letters "A". Note that $\varepsilon(s)$, δ and ϕ can be found by recursive training on a set of similar primitives.

2.3 Hierarchical Structure of 2-D Patterns

Differential structure provides partial, but crucial, information about handwritten letters. For complete characterization of the letters, the length ratios and coordinate frames must be considered. We define the curve segment as a partition of the image outline between two neighboring vertices. Thus the length ratio is given by the length of a curve segment divided by the length of the longest curve segment. This idea applied to a group having similar differential structure can further classify the group into subgroups.

The primitives "**H**" and "**I**" have the same properties in differential structure. The distinctions between them are length ratio and their orientation in the coordinate frame. If the referenced coordinate frame is rotated, the number of local extrema on both $x(t)$ and $y(t)$ [image outline $f(t) = (x(t), y(t))$] changes. It appears that $f(t)$ is dependent on the coordinate and it is useful to the classification of pattern orientation, such as "**6**" and "**9**" or "**X**" and "**+**". Fig. 7 shows the hierarchical structure of patterns. The hierarchical structure provides the main information for pattern recognition.

3. Implementation and Results

This section discuses the above idea for digital implementation. Fig 8 shows three scanned handwritten symbols with 150 dots per inch (DPI) resolution. The video images (16 gray levels) are segmented using the correlation thresholding method (Brink 1989), and enhanced by removing noise (Gonzalez and Woods 1992). After the preprocessing, the pictures have only two values (black and white) and each picture has only one image primitive. Our discussion begins with given such image primitives. (Note: For convenience in later discussion, the left image of Fig 8 is named *boy1*, the middle named *boy2*, the right named *boy3*).

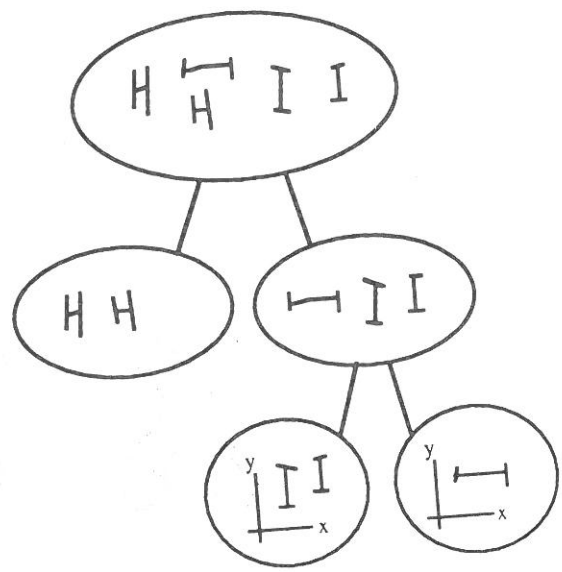

Fig. 7. Hierarchical Structure of Patterns

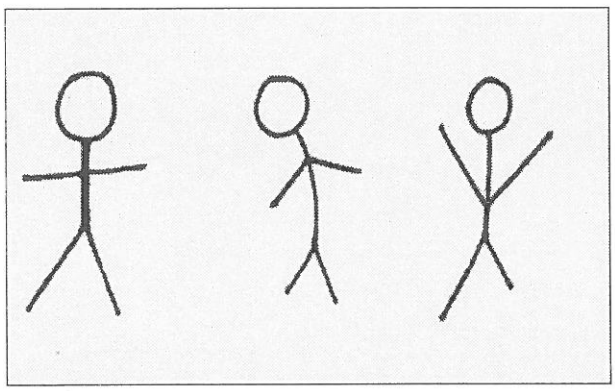

Fig. 8. Three handwritten boys

3.1 Contour Tracing

An image outline is a description of an object's boundary; e. g. a series of black points on the boundary of a white object against a black background. The algorithm can be found in Stallings' paper (1977). Keeping the black region (object) on the right hand side, we proceed tracing along the outline of an object from point to point, turning left after encountering a while point and right after a black point. This is depicted in Fig 9. Fig 10 shows the result of detecting the boundary of *boy1*.

3.2 Digital Differential Calculus

The digital image outline then is $\mathbf{f}(t_i) = (x(t_i), y(t_i))$, where t_i is an integer. Then the numerical formulas for normalized first and second derivative of the function $\mathbf{f}(t_i)$ are given by:

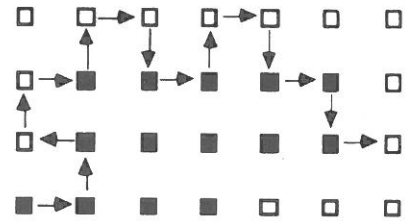

Fig. 9. Contour Tracing

Note that the vector $(x'(t_i), y'(t_i))$ is a unit vector.

3.3 Reparameterization and Error

The method of reparameterization is to use $x'(t_i) = 0$ and $y'(t_i) = 0$ (or in terms of digital calculation $-\delta \leq x'(t_i) \leq +\delta$, $-\delta \leq y'(t_i) \leq +\delta$) so that corner points can be found to adjust the parameter of each segment between two neigbouring convex points or corner points. The

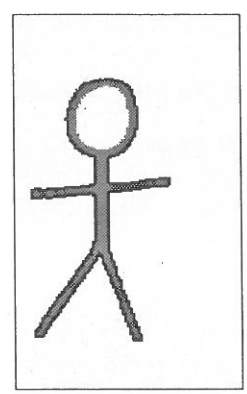

Fig. 10. Detecting the image outline of *boy1*

$$x'(t_i) = \frac{x(t_{i+1}) - x(t_{i-1})}{\sqrt{(x(t_{i+1}) - x(t_{i-1}))^2 + (y(t_{i+1}) - y(t_{i-1}))^2}}$$

$$y'(t_i) = \frac{y(t_{i+1}) - y(t_{i-1})}{\sqrt{(x(t_{i+1}) - x(t_{i-1}))^2 + (y(t_{i+1}) - y(t_{i-1}))^2}}$$

$$x''(t_i) = \frac{\dfrac{x(t_{i+1}) - x(t_i)}{\sqrt{(x(t_{i+1}) - x(t_i))^2 + (y(t_{i+1}) - y(t_i))^2}} - \dfrac{x(t_i) - x(t_{i-1})}{\sqrt{(x(t_i) - x(t_{i-1}))^2 + (y(t_i) - y(t_{i-1}))^2}}}{\sqrt{\left(\dfrac{x(t_{i+1}) - x(t_{i-1})}{2}\right)^2 + \left(\dfrac{y(t_{i+1}) - y(t_{i-1})}{2}\right)^2}}$$

$$y''(t_i) = \frac{\dfrac{y(t_{i+1}) - y(t_i)}{\sqrt{(x(t_{i+1}) - x(t_i))^2 + (y(t_{i+1}) - y(t_i))^2}} - \dfrac{y(t_i) - y(t_{i-1})}{\sqrt{(x(t_i) - x(t_{i-1}))^2 + (y(t_i) - y(t_{i-1}))^2}}}{\sqrt{\left(\dfrac{x(t_{i+1}) - x(t_{i-1})}{2}\right)^2 + \left(\dfrac{y(t_{i+1}) - y(t_{i-1})}{2}\right)^2}}$$

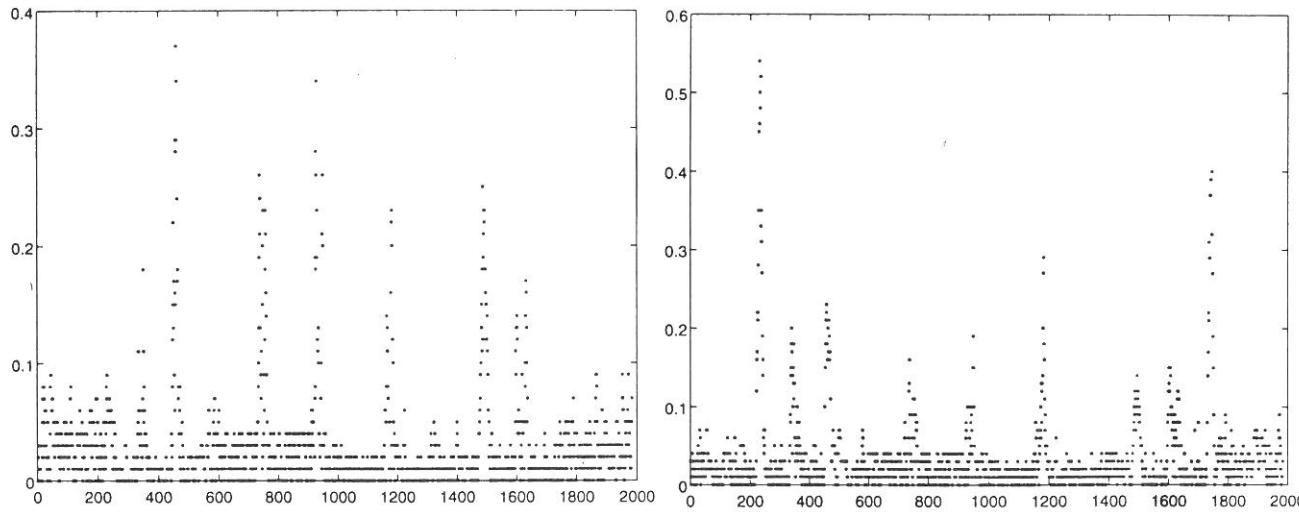

11.a: $|\mathbf{N}_{\text{boy1}}(s_i) - \mathbf{N}_{\text{boy2}}(s_i)| = \varepsilon(s_i)$

11.b: $|\mathbf{N}_{\text{boy1}}(s_i) - \mathbf{N}_{\text{boy3}}(s_i)| = \varepsilon(s_i)$

Fig. 11. Point comparison

convex points correspond to curvature $\neq 0$. Detecting the corner points is still a problem (Teh and Chin 1989) (Rattarangsi and Chin 1992), although in our examples the corner points are obvious with respect to the scale.

Fig. 11a and 11b shows

$$|\mathbf{N}_{\text{boy1}}(s_i) - \mathbf{N}_{\text{boy2}}(s_i)| = \varepsilon(s_i)$$

and

$$|\mathbf{N}_{\text{boy1}}(s_i) - \mathbf{N}_{\text{boy3}}(s_i)| = \varepsilon(s_i).$$

Note that the error is obtained from the difference between two unit vectors so the vertical exis shows the error value which is between 0 and 2. The horizontal axis gives points along the image outline appropriately scaled (about 2 000 points). It appears that some error values are quite high due to the legs and arms of the images *boys* having different angles. As mentioned before, setting different error values for these regions is necessary.

Using the concept of neighborhood,

$$\min_j\{|\mathbf{N}_{\text{boy1}}(s_i) - \mathbf{N}_{\text{boy2}}(s_j)|\} = \varepsilon(s_i)$$

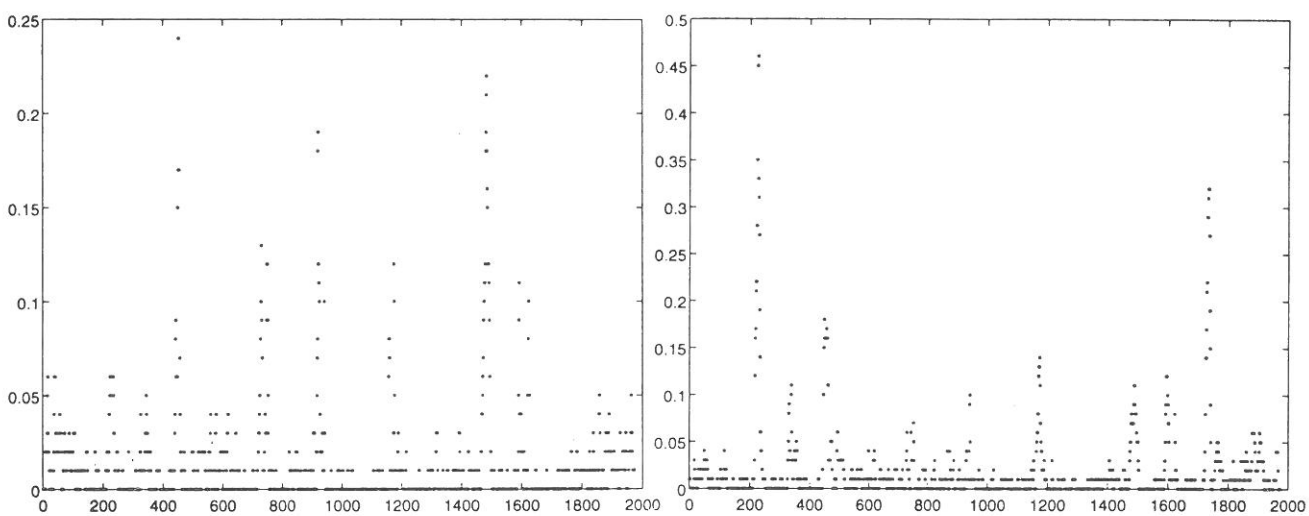

12.a: $\min_j\{|\mathbf{N}_{\text{boy1}}(s_i) - \mathbf{N}_{\text{boy2}}(s_i)|\} = \varepsilon(s_i)$

12.b: $\min_j\{|\mathbf{N}_{\text{boy1}}(s_i) - \mathbf{N}_{\text{boy3}}(s_i)|\} = \varepsilon(s_i)$

Fig. 12. Neighborhood comparison

and

$$\min_j\{|\mathbf{N}_{\text{boy1}}(s_i) - \mathbf{N}_{\text{boy3}}(s_j)|\} = \varepsilon(s_i)$$

where $s_j \in (s_{i-5}, s_{i+5})$. We obtain better results as shown in Fig 12a and 12b.

In order to classify the patterns of the three boys, we can set the ε functions in accordance with $|\mathbf{N}_{\text{boy1}}(s_i) - \mathbf{N}_{\text{anyboy}}(s_i)| + \delta$, where δ is a small value corresponding to the change in the arms or legs of a boy. For example, to distinguish *boy3* with arms raising from *boy1* and *boy2* with arms not raising, ε function should be set as $|\mathbf{N}_{\text{boy1}}(s_i) - \mathbf{N}_{\text{boy2}}(s_i)| + \delta$. If a boy has only one arm, so that its number of convex points is different to that of a boy with two arms, this primary information filters out disabled boys (i. e. a leg or arm). Considered with general techniques of pattern recognition, distinguishing different image patterns is easier than grouping similar patterns.

Our method was applied to a practical application of the automated vote counting problem with emphasis on the application of pattern recognition. We successfully identified simple vote markings such as crosses ("**X**" and "+"), ticks, circles, rectangles and asterisks (Lui 1992). Fig 13 illustrates two different samples of ballot sheets.

4. Related Work: Generalized Hough Transform

A shape matching technique based on the straight line Hough transform has been described by Pao et al (1992). Conceptually, each point in $\theta - \rho$ space corresponds to a line that is tangent to the curve. A second transform, which is a signature of the shape, is computed by measuring the perpendicular distances between pairs of parallel tangent lines. To recognize a test object, it is only necessary to compute a 1-D correlation of the signature with the normalized reference signature.

In contrast with the above method, our method is concerned completely with geometric feature extraction. It is proved that a continuous closed, smooth curve is indeed uniquely characterized by its complete set of tangents (Pao et al 1992). This, in turn, is a problem of understanding the set of tangents. We have presented it as the interpretation of geometric properties.

The Hough transform method has the same advantages as ours, such as position, orientation and scale independence. Another advantage of the Hough transform approach is the use of correlation for recognition based on 1D vectors instead of 2D templates. In our method, the correlation of $\kappa(s)$ can be used to describe the matching. However, it is better to use the ε function

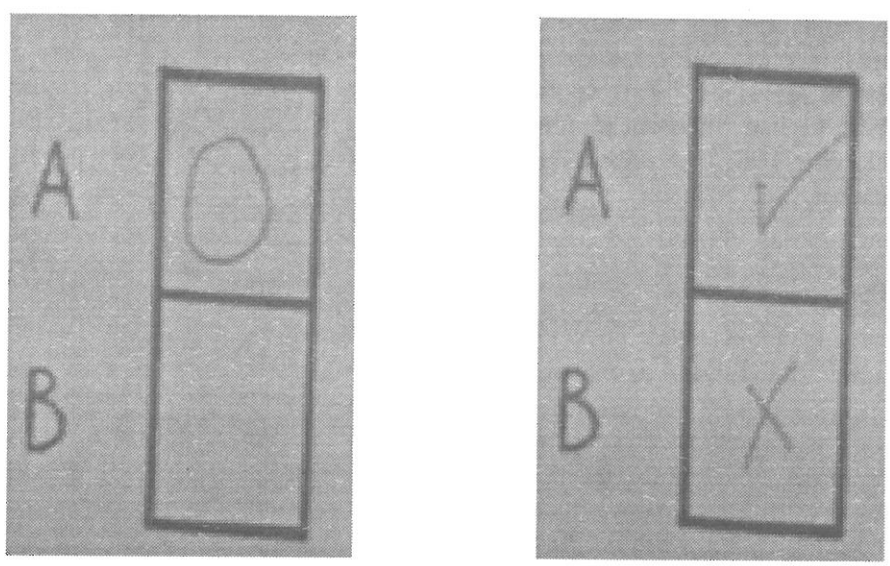

Fig. 13. Examples of ballot papers (scanned image)

because the image outlines have been standardized in rough. Furthermore, the ε function can highlight some critical sections for recognition.

Since each point in $\theta - \rho$ space corresponds to a line that is tangential to the curve, the Hough transform method will suffer difficulties when the image has many shape outline vertices or high curvature. Many overlapping lines will result in the $\theta - \rho$ space, possibly affecting the correlation test for recognition of the object (Fig 14). With the method described in this paper, more vertices simply provide detailed information and thus it works well since a computer program can detect the outline vertices efficiently.

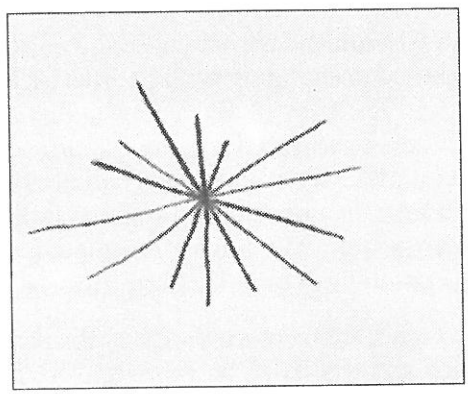

Fig. 14. The outline of an asterisk image contains many outline vertices, which result in more curves after Hough Transformation.

One major disadvantage of this method is recognition of a bad handwritten pattern. The problem is obviously that bad handwritten patterns change geometric shape locally, but the global structure would be the same. Part of our ongoing research is to use differential topology (Brocker and Janich 1982) to understand the structure of patterns.

5. Mummy Method

This section shows the linkage of the previous 2D method with 3D object recognition. The simplest method for identification of a 3-D object exploits its three orthogonal profile views: front view, side view and back view. Each view becomes a 2-D pattern recognition problem similar to those above. However, given a 3-D object, how do we define the "front view"? (Note: once the front view is known, the top and side can be determined by their orthogonal relationships). This problem is crucial since the front view of an object should be comparable with the corresponding view of any other object, although in certain cases, especially complicated objects, a single significant angle of view can decisively identify the object, for example the front view of a human shape. One possible choice of front view is that view which has maximum area enclosed by its profile boundary outline.

People used to think that the earth was flat. Later, through observation and calculation, they determined that the earth was round. Similarly, general relativity pointed out that the universal space was neither flat nor 3–dimensional, but curved and 4–dimensional. The problem of object recognition parallels these examples. Curve theory applied to 2-D pattern recognition can be extended to 3-D cases. Object recognition can be formulated in terms of recognizing a long, helix–like curve around an object's surface (like wrapping a mummy). In this section, we propose the "*mummy method*" whereby a finite curve encapsulates the 3-D shape.

The mummy method can be thought of as using a long line wrapped spirally round an object. Thus, the line looks like a helix (Fig 15). An object is a 2-D manifold M 4mbedding in $\mathbf{R}^3$. Let $\mathbf{f} : \mathbf{R} \rightarrow \mathbf{R}^3$ such that $\mathbf{f}(t) = (x(t), y(t), ht) \in \mathbf{M}$, where $h > 0$. This is called a right helix. (If $h < 0$ it would be a left helix).

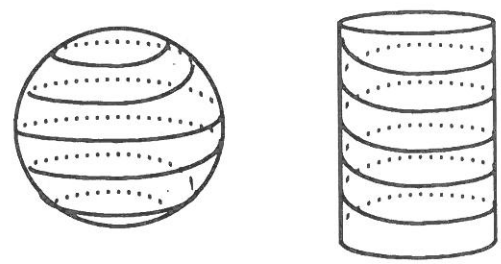

Fig. 15. A helix–like curve around an object's surface, like wrapping a mummy, can provide sufficient information about the object.

The starting point for wrapping an object should be chosen at one end of the longest axis through the object. Set the longest axis as z axis. Thus a starting point will be a

$(x(t), y(t), 0)$. $\mathbf{f}(t)$ is found by contour tracing at each constant level of z–axis. Each contour tracing of $f(x(t), y(t), h)$, where h is constant from 0 to the length L of an object along z–axis, is different from 2-D since the data is sparse. We make an assumption that the next point $(x(t_{n+1}), y(t_{n+1}), h)$ is the nearest point of $(x(t), y(t), h)$ and it is not the same as previous detected pointed, i. e. $(x(t_{n+1}), y(t_{n+1}), h) \notin \{(x(t_n), y(t_n), h), (x(t_{n-1}), y(t_{n-1}), h), \ldots\}$. Once it finishes a circular route, h will increase to another layer until it reaches the final value of the longest axis z. Although the discrete version of $\mathbf{f}(s)$ being $\{\mathbf{f}(s_0), \mathbf{f}(s_1), \ldots, \mathbf{f}(s_n)\} = \{(x(t_0), y(t_0), 0), (x(t_1), y(t_1), 0), \ldots, (x(t_{l_0}), y(t_{l_0}), 0), (x(t_0), y(t_0), 1), \ldots, (x(t_{l_1}), y(t_{l_1}), 1), \ldots, (x(t_{l_n}), y(t_{l_n}), L)\}$ could not be easily visualized as a helix–like curve, it in fact is a high–looped helix. Note $\mathbf{f}(s)$ is a finite curve. Different helix curves can be compared with each other if we reparameterize the $h(s)$ of $\mathbf{f}(s)$ in a unit.

Once $\mathbf{f}(s)$ is found, the problem is similar to the previous sections. In Fig 16, we plot the resulting reparameterized curves $x(s)$ against for a sphere and a cylinder, respectively. The two curves clearly reflect the geometric shapes of the sphere and the cylinder. Most importantly, $\mathbf{f}(s)$ is not dependent on any coordinates.

Although the mummy method is appealing as it is a simple way to analyze an object, the approach must have three dimensional image data. Besel and McKay (1992) propose a general purpose method for registration of 3-D shapes including free–form curves and surfaces. Their free–form shape matching method is very useful as a part of our method.

6. Conclusions

An image file consists of discrete data. A theory based on the assumption of continuity may yield an incorrect result. This happens mostly in the theory of image processing, such as Fourier transformation, gradient operations and the like. Certainly it can be solved by numerical analysis; however, it complicates the whole implementation.

We have indicated some conclusions and limitations in the previous sections. The future work regarding this approach is twofold. Firstly, the combination of the geometric properties and differential topological structure of bad handwritten image primitives is our main current interest. One can write a letter in diverse ways; however, the differential topological structure of a set of "A"s is preserved.

Secondly, the mummy method could be extended to the recognition of complex objects.

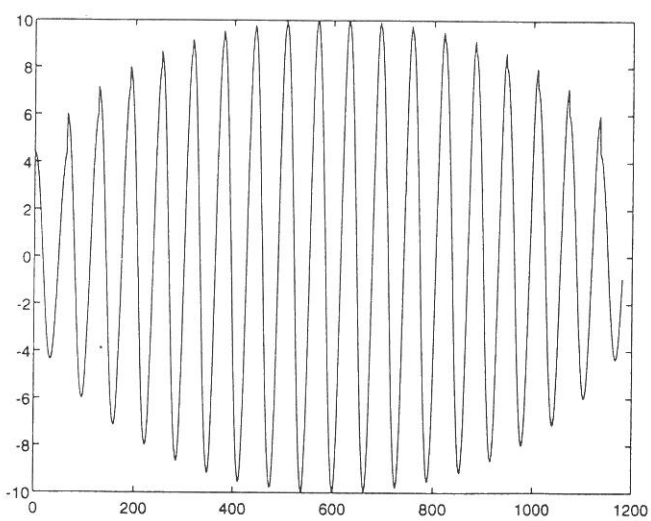

16.a: Curve $x(s)$ on sphere

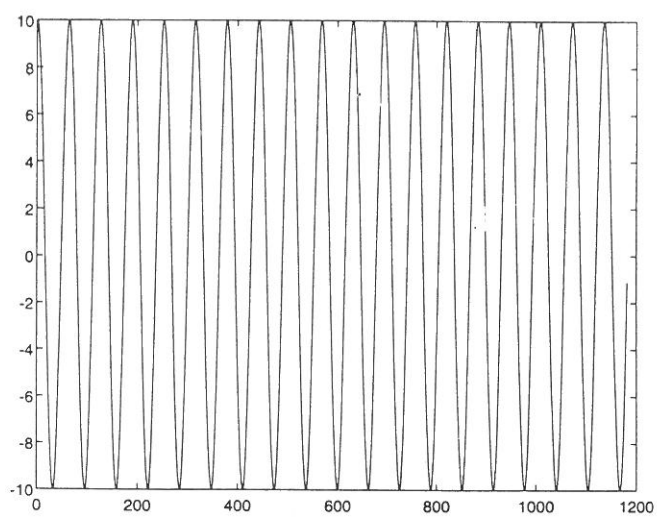

16.b: Curve $x(s)$ on cylinder

Fig. 16. Both curves reflect the geometric shapes of the sphere and the cylinder.

It is important to notice that, (Seibert and Waxman, 1992), the popular approach of 3-D recognition system based on the imagery is to hypothesize an object using view information. It then generates the object's expected appearance in order to test the degree of matching. We would like to combine the idea of the mummy method and the knowledge–based model to develop our method from 2-D views.

Acknowledgment. The authors are grateful to two anonymous referees for their helpful comments on this paper.

References

P. J. BESL AND N. D. MCKAY A method for Registration of 3-D Shapes, *IEEE Transactions on Pattern Analysis and Machine Intelligence*, Vol 14, No. 2. (1992), 239–256.

A. D. BRINK Grey–level thresholding of images using a correlation criterion, *Pattern Recognition Letters* 9 (1989), 335–341.

T. H. BROCKER AND K. JANICH *Introduction to Differential Topology*. Cambridge University Press, Great Britain, 1982.

R. C. GONZALEZ AND R. E. WOODS *Digital Image Processing*, Addison–Wesley, 1992.

K. M. LUI Categorization and Spoilt Votes Analysis: A Geometric View of Pattern Recognition, *Proceedings of the Third South African Workshop on Pattern Recognition*, Johannesburg, (1992), 89–96.

D. C. W. PAO, H. F. LI AND R. JAYAKUMAR Shapes Recognition Using the Straight line Hough Transform: Theory and Generalization, *IEEE Transactions on Pattern Analysis and Machine Intelligence*, Vol 14, No. 11 (1992), 1076–1089.

A. RATTARANGSI AND R. T. CHIN Scale–Based Detection of Corners of Planar Curves, *IEEE Transactions on Pattern Analysis and Machine Intelligence*, Vol 14, No. 4 (1992), 430–449.

M. SEIBERT AND A. M. WAXMAN Adaptive 3-D Object Recognition from Multiple Views, *IEEE Transactions on Pattern Analysis and Machine Intelligence*, Vol 14, No. 2 (1992), 107–124.

M. SPIVAK *A Comprehensive Introduction to Differential Geometry* (Volume II), second edition, Publish or Perish, Inc. Berkeley, 1979.

W. W. STALLINGS Chinese Character Recognition, *Syntactic Pattern Recognition Applications*, edited by K. S. Fu, Springer–Verlag, 1977.

F. STEIN AND G. MEDIONI Structural Indexing: Efficient 3-D Object Recognition, *IEEE Transactions on Pattern Analysis and Machine Intelligence*, Vol 14, No. 2 (1992), 125–144.

C. TEH AND R. T. CHIN On the Detection of Dominant Points on Digital Curves, *IEEE Transactions on Pattern Analysis and Machine Intelligence*, Vol 11, No. 8 (1989), 859–872.

Received: May, 1993
Accepted: October, 1993

Contact address:

Kim Man Lui
Department of Computer Science
University of the Witwatersrand
Private Bag 3, PO Wits 2050
Johannesburg, South Africa
Email: kimman@concave.cs.wits.ac.za
Fax: 27-11-3397965

Anton Brink
Department of Computational and Applied Mathematics
University of the Witwatersrand
Private Bag 3, PO Wits 2050
Johannesburg, South Africa
Email: 076anton@witsvma.wits.ac.za
Fax: 27-11-3397965

Michael Sears
Department of Computational and Applied Mathematics
University of the Witwatersrand
Private Bag 3, PO Wits 2050
Johannesburg, South Africa
Email: 076sears@witsvma.wits.ac.za
Fax: 27–11–3397965

KIM MAN LUI recieved the B. Eng. in 1990 from Tamkang University, Taiwan. Since 1992, he has been awarded a scholarship to study for his M. Sc. in computer science at the University of the Witwatersrand, South Africa. Mr Lui has been invited to be the chairperson for the hardware session of the Asian Conference on Computer Vision 1993, Japan.

ANTON DAVID BRINK received an M. Sc. From Rhodes University in 1987. He is currently employed as a lecturer in the Department of Computational and Applied Mathematics at the University of the Witwatersrand while studying towards a Ph. D. His research interests are in the application of the Maximum Entropy formalism to unsupervised image segmentation and modeling of digital images.

MICHAEL SEARS is Professor in the Department of Computational and Applied Mathematics at the University of the Witwatersrand, Johannesburg. His main interest is in the theory of dynamical systems, but he is also involved with the group in Image Processing and this led to several joint publications.